Optimal Control Theory applied to Unintended Source Control and Field Shaping for Time-Harmonic Electromagnetic Waves

Maxime Spirlet, *Member, IEEE,* Christophe Geuzaine, *Member, IEEE* and Véronique Beauvois, *Member, IEEE*

***Abstract*—This paper addresses the experimental control of time-harmonic electromagnetic waves. The underlying optimal control problem aims to find a set of values to apply to control sources, located in the controlled region or on its boundary, allowing any electromagnetic field caused by an undesired noise source to be suppressed or replaced by any other field map. After a presentation of the control method, illustrated with a few numerical applications, two experimental setups are considered. The first setup aims to control the voltage within a mixed microstrip/coaxial transmission line. In the second setup, the electric field inside a cross-shaped waveguide network is controlled. For both setups, the working frequency is chosen in the UHF range and a comparison is made to the results given by the equivalent numerical models.**

***Index Terms*—Optimal control, electromagnetic waves, noise cancellation, field shaping, *in-situ* testing.**

I. Introduction

CONTROLLING electromagnetic environments to replace an undesired field map by another field map in a region of interest is a challenging task, which can be seen as active noise control for electromagnetic waves, and could be particularly useful where low field zones are required without using any electromagnetic shielding. This technique can not only be applied to control conducted or radiated noise but also to shape electromagnetic fields to arbitrary needs. This approach is thus particularly suited for *in-situ* electromagnetic compatibility tests where ambient noise reduction and accurate generation or measurement of radiation levels are critical but nevertheless difficult to reach due to the particular conditions of the test environment. *In-situ* test environment are indeed generally partially or weakly reverberating environments, preventing the confident use of classical test methods built for (semi or full) anechoic environments or fully reverberating environments (mode stirred reverberation chambers for example).

Assuming that noise has been quantified by any mean, the general mathematical framework commonly used to deal with time domain control problems is the Hilbert Uniqueness Method (HUM) [1]. Besides proving the existence and unicity of the solution to the problem of finding the control values (either distributed within the controlled region or located on its boundary) driving a perturbed system to rest after a sufficiently large period of time T, this framework also provides a way to compute those control values using the HUM operator, as demonstrated numerically for time domain acoustic and electromagnetic wave problems [2]–[4]. Unfortunately, numerical simulations have shown that the discrete HUM operator is built in such a way that it is highly sensitive to small variations, which makes it unsuited to use experimentally. Robust alternative methods, more suited to experimental conditions, also exist for pulsed regime, but are rather devoted to highly reverberating environments (e.g. [5]–[7]).

In the context of electromagnetic compatibility applications, we are interested in harmonic or repetitive pulse noise perturbations in general environments (not necessarily highly reverberating), where time-harmonic methods are more interesting than time-oriented control approaches. Moreover, the control to apply is also becoming time-independant, which facilitates practical experiments.

In this work, we thus consider a time-harmonic control method, with the major advantage that noise is stationary. Although the HUM framework is still applicable [8], it is not mandatory since the system does not need to be driven to rest, and does not depend on time. More classical and more robust optimization methods for elliptic problems can thus be employed [9]–[12]. Moreover, a boundary control is also preferred to keep the controlled environment unmodified. The control can be limited to a part of the boundary of the controlled region depending on its topology [13].

Basically, controlling a region in the frequency domain implies to find the amplitude and phase of each control source that will cancel the field generated by the undesired source(s) in this region. The use of an array of transducers approximating an equivalent surface bounding a domain where to control noise has been developed for active electromagnetic cloaking. The equivalent Love's (Schelkunoff's) surface has been used to perform some active cloaking in free-space by generating the sources needed to compensate the scattered field caused by an object [14]. Other techniques of active shielding using polynomial approximation for Laplace and Helmholtz equations [15] have also been developed. Using the UHF range is rather uncommon in active cloaking [16], and higher frequencies are generally encountered in the literature [17]. However, those solutions are only limited to free-space and are not suited for reverberating and/or complex environments.

The idea developed in this paper relies on optimal control theory [3], rather than on the equivalence principle, for the time-harmonic electromagnetic wave, but is this time usable for any complex and/or reverberating environment. If the region is a single point, cancelling the field is easily achieved

The authors are with the Montefiore Institute, Department of Electrical and Computer Engineering, University of Liège, Belgium (e-mail: maxime.spirlet@uliege.be).

with a control source having the proper amplitude and phase delay, but if the region is larger, the control sources weights (amplitude and phase) have to be chosen to compensate the source field exactly on the whole region, which is generally unfeasible. As a result, an optimum in the applied control values has thus to be found to fit the target field at best, i.e. according to a given norm on the domain.

In this paper, the experimental control of time-harmonic electromagnetic waves is addressed for different practical situations. Although several numerical results are available for the optimal control of elliptic problems, this paper is, to the best of our knowledge, one of the first to propose such equivalent experimental applications and results for electromagnetic UHF systems. In Section II, the principles of the applied optimization method to find the optimal control values is described, as well as a possible method to estimate the perturbation to be compensated. Some numerical illustration of the control method applied to some idealized experimental configurations are presented in Section III. In Section IV, two different simple albeit non trivial experimental control test cases are proposed, followed by a discussion comparing the experimental results and the results provided by an equivalent numerical model. Some conclusions are finally drawn in the last section.

II. Optimal Control Principles

The generic problem to solve in a domain Ω, depicted in Fig. 1, consists in finding the appropriate control values $\vec{u}$ distributed in a region $\Omega_c \subset \Omega$ which surrounds the observation region $\Omega_o \subset \Omega$ where a desired target electric fields E_o is saught, whereas the source $\vec{f}$ located in $\Omega \setminus \Omega_c$ generates an electric field $\vec{E}_f$ in the whole domain Ω. This is equivalent to minimizing the energy functional

$$J(\vec{E},\vec{u}) = \frac{1}{2}\int_{\Omega_o} \left\| \vec{E}(x) - \vec{E}_o(x) + \vec{E}_f(x) \right\|^2 d\Omega + \frac{\lambda}{2}\int_{\Omega_c} \left\| \vec{u}(x) \right\|^2 d\Omega, \quad (1)$$

where $\vec{E}$ is the state function (i.e. the electric field, depending on the location $\vec{x}$), The solution $(\vec{E},\vec{u})$ needs to be restricted using appropriate constraints pertaining to the physics of the problem, i.e.:

$$\left\{ \begin{array}{rcll} \nabla\times\nabla\times\vec{E} - k^2\vec{E} &=& \vec{u}\mathbb{1}_{\Omega_c} & \text{on} \quad \Omega \\ \vec{n}\times\vec{E} &=& 0 & \text{on} \quad \partial\Omega, \end{array} \right. \quad (2)$$

where k is the wave number, $\mathbb{1}_{\Omega_c}$ is the indicator function in Ω_c, and $\vec{n}$ is the exterior unit normal to $\partial\Omega$, the boundary of Ω.

The objective functional J in (1) consists in two terms: the first one ensures that the resulting field after control will get as close to the target function as possible (in L_2 norm) while the second one has a regularizing effect by measuring the cost of the applied control. The parameter λ has to be chosen such that $|\lambda| \geq 0$, but preferably $|\lambda| > 0$ to avoid singular or *bang-bang* controls [18]. The target function $\vec{E}_o$ should also be solution of the wave equation and interestingly encompasses either a null field or any other pattern such as spherical or plane waves. The target field map is limited to Ω_o which is surrounded by the distributed control Ω_c. Using a distributed control located around the region to control (Ω_o) is preferred rather than placing the control on the boundary of Ω since in practice, we are more likely to encounter that kind of configuration (in free-space for example). The constraint (2) is the classical time-harmonic vectorial wave equation assorted with a homogenous Dirichlet boundary condition. For the sake of clarity, we have used a homogenous Dirichlet condition, but any other valid boundary condition could be chosen.

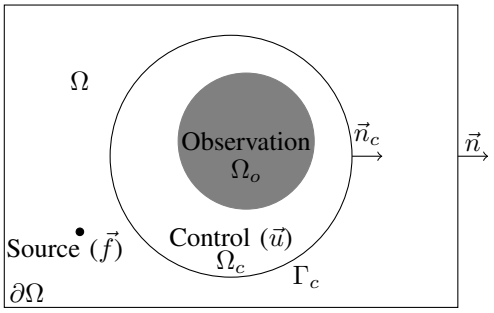

Fig. 1. Generic configuration for the optimal control of the electric field in the Ω_o region.

To solve the optimization problem $\min J(\vec{E},\vec{u})$, we propose to express the optimality conditions [19] (see also [20]–[22] for existence and uniqueness of solutions):

$$\left\{ \begin{array}{lll} \nabla\times\nabla\times\vec{E} - k^2\vec{E} = \vec{u}\mathbb{1}_{\Omega_c} & \text{on} & \Omega \\ \nabla\times\nabla\times\vec{p} - k^2\vec{p} = \left(\vec{E} - \vec{E}_o + \vec{E}_f\right)\mathbb{1}_{\Omega_o} & \text{on} & \Omega \\ \vec{u} = \vec{p}/\lambda & \text{on} & \Omega_c \end{array} \right. \quad (3)$$

with $\vec{p}$ the associated Lagrange multiplier variable defined in Ω [19].

By applying the weighted residuals method on each equation of (3), a variational form is found, allowing to solve the optimization problem numerically using the Finite Element Method (FEM): find $\vec{p}$, $\vec{u}$ and $\vec{E}$ such that

$$\left\{ \begin{array}{rl} -\displaystyle\int_\Omega \left(\nabla\times\vec{p}\right)\cdot\left(\nabla\times\vec{p'}\right)\, d\Omega + k^2\int_\Omega \vec{p}\cdot\vec{p'}\, d\Omega & \\ \qquad + \displaystyle\int_{\Omega_o}\left(\vec{E} - \vec{E}_o + \vec{E}_f\right)\cdot\vec{p'}\, d\Omega_o &= 0 \\ \lambda\displaystyle\int_{\Omega_c}\vec{u}\cdot\vec{u'}\, d\Omega_c + \int_{\Omega_c}\vec{p}\cdot\vec{u'}\, d\Omega_c &= 0 \\ -\displaystyle\int_\Omega \left(\nabla\times\vec{E}\right)\cdot\left(\nabla\times\vec{E'}\right)\, d\Omega + k^2\int_\Omega \vec{E}\cdot\vec{E'}\, d\Omega & \\ \qquad + \displaystyle\int_{\Omega_c}\vec{u}\cdot\vec{E'}\, d\Omega_c &= 0 \end{array} \right. \quad (4)$$

hold for all appropriate test functions $\vec{p'}$, $\vec{u'}$ and $\vec{E'}$ [23].

However, it has been assumed that the field map $\vec{E}_f$ generated by $\vec{f}$ in the observation region Ω_o was known, which is generally not the case. Furthermore, sampling the whole controlled domain Ω_o is neither realistic nor practical. If the control region Ω_c is homogenous (or more generally if the Green function of the solution is known), one can apply the sampling on its boundary Γ_c, using the Stratton-Chu integral

formula [24]:

$$\vec{E}(\vec{x}) = \int_{\Gamma_c} \jmath\omega\mu \left(\vec{n}_c \times \vec{H}\right) \mathcal{G} + \left(\vec{n}_c \times \vec{E}\right) \times \nabla\mathcal{G} + \left(\vec{n}_c \cdot \vec{E}\right) \nabla\mathcal{G}\, dS. \quad (5)$$

In the following, we assume that Ω_c is in free space, where the corresponding Green's functions in 2D and 3D read respectively:

$$\mathcal{G}_{3D} = \frac{e^{\jmath kr}}{4\pi r}, \quad \mathcal{G}_{2D} = \frac{\jmath}{4}\mathcal{H}_0^1(kr). \quad (6)$$

Note that in an experimental setup, using (5) implies to measure the value of the magnetic field (or at least $\nabla \times \vec{E}$) which is a rather difficult task in the Ultra High Frequency (UHF) range. For numerical purposes, the integral in (5) is computed using a numerical quadrature on N_c points. In our setups we chose Γ_c as a circle of radius r_c and use the trapezoidal integration rule, which leads to spectral convergence:

$$\tilde{\vec{E}}_f = \sum_{i=1}^{N_c} \left(\jmath\omega\mu \left(\vec{n}_c \times \vec{H}\right)_i \mathcal{G}_i + \left(\vec{n}_c \times \vec{E}\right)_i \times \nabla\mathcal{G}_i + \left(\vec{n}_c \cdot \vec{E}\right)_i \nabla\mathcal{G}_i\right) \Delta S_i \quad (7)$$

It is also interesting to emphasize that controlling using the whole boundary Γ_c is a sufficient but not necessary condition. Based on the source to cancel and the geometry (topology), applying the control to a part of the boundary might be sufficient to guarantee the exact control [13], by respecting the Geometric Control Condition (GCC). As a result in 1D, the control can interestingly be applied in only 1 or 2 points.

The optimality condition (4) can now be solved to find the best $\vec{u}$ that will produce the required field $\vec{E}_o$ in the controlled zone Ω_o. In the next section, we propose some numerical results to illustrate the method presented above.

III. Numerical Illustrations

For all the presented numerical results, the implementation of the optimization method has been achieved using the FEM solver GetDP [25]. The geometries and post-processing were obtained using Gmsh [26].

A. Electric field control in free-space

For the first test case, we have applied the method to a free-space region having a disturbing source whose resulting field has to be cancelled in a determined zone. It is in fact a straightforward implementation of the problem described in Fig. 1. A Perfectly Matched Layer (PML) has nonetheless been introduced around the domain Ω to model infinity and to approximate free-space radiation conditions. The exact configuration of the problem is depicted in Fig. 2. The control part consists of 64 point sources distributed around the zone to be controlled. We have chosen to impose two different well-known fields $\vec{E}_o$ to illustrate the method. The former is a zero-field zone and the latter is a plane wave propagating in the $\vec{x}$ direction. The UHF harmonic source $\vec{f}$ was fixed at 1 GHz.

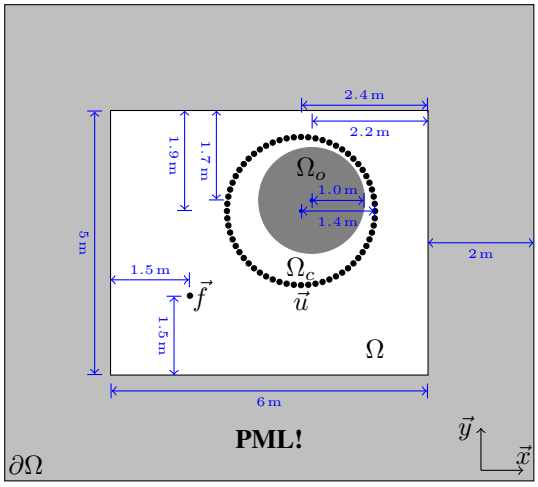

Fig. 2. Configuration of test case 1.

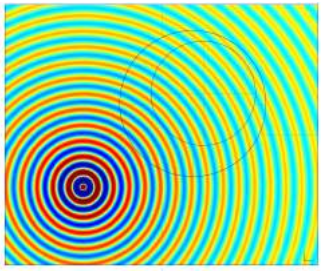

(a) Without control

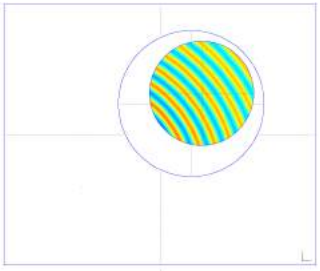

(b) Reconstructed source field in Ω_o

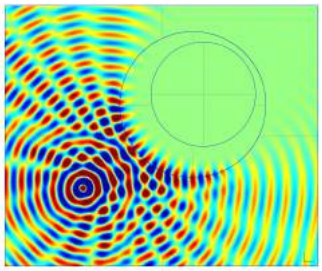

(c) With control: null field, exact source

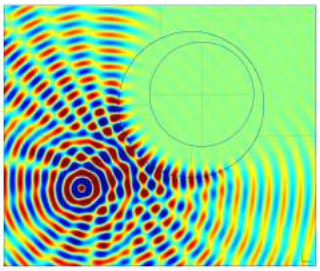

(d) With control: null field, reconstructed source

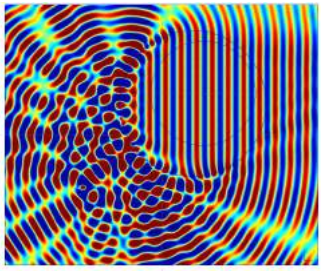

(e) With control: plane wave, exact source

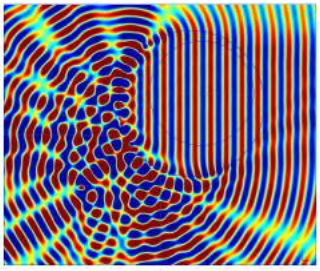

(f) With control: plane wave, reconstructed source

(g) Field scale

Fig. 3. Test case 1: 2D control in free-space of the electric field in a target zone using either the exact source field $\vec{E}_f$ ((c),(e)) or the reconstructed field $\tilde{\vec{E}}_f$ ((d),(f)) using 64 sample points.

The results of the test case 1 are shown in Fig. 3. The resulting field caused by the source $\vec{f}$ is plotted in Fig. 3a. The reconstructed field $\tilde{\vec{E}}_f$ using (7) with 64 samples (from the same control points Ω_c) is displayed in Fig. 3b. The spatial sampling with 64 values distributed along a circle of radius $1.4\,\mathrm{m}$ respects the sampling criterion of $\lambda/2$ [27]. The reconstructed field $\vec{E}_f$ is pretty accurate: only a slight phase shift is noticeable when the original and the reconstructed fields are superposed, merely caused by the inherent FEM phase error (using a smaller mesh size decreases significantly the phase shift). Figs. 3c and 3d show the total field after applying the control method with, on the left, the resulting field map using the exact field $\vec{E}_f$ and, on the right, the resulting field using the reconstructed field $\tilde{\vec{E}}_f$. In both cases, in the region Ω_o the electric field is reduced significantly. The resulting field using the reconstructed field is a bit worse than with the exact field. This was expected since the reconstructed field is slightly different compared to the original field, causing the computed control values $\vec{u}$ to be optimal, but only for the reconstructed source field, not the true one. Figs. 3e and 3f exhibit exactly the same behavior: the plane wave is accurately generated in the region Ω_o, with a slight deterioration in the case where the reconstructed field $\tilde{\vec{E}}_f$ is used, for the same reasons mentioned above.

The errors between the obtained fields and the target fields have not been quantified here as this paper is mainly devoted to the experimental application of the presented method, already implying significant measurement errors compared to numerical reconstruction errors.

B. Electric field control in a cavity

For test case 2, a two dimensional room, described in Fig. 4 is considered. In addition to test case 1, boundary walls have been placed around the region Ω. Those walls have a composition comparable to concrete, with a relative permittivity $\epsilon_r = 8$ and conductivity $\sigma = 1 \times 10^{-4}\,\mathrm{S}$. This discontinuity between the air and the walls causes some reflections, which are complexifying the field map inside the room. The rest of the configuration is exactly the same as in test case 1.

As seen in Fig. 5, the resulting field after applying the control is accurately matching the target field $\vec{E}_o$. Despite the reverberating environment, the presented method is able to find the control value to apply in the region Ω_c to generate the desired electric field in the region Ω_o. Considering the reconstructed field $\tilde{\vec{E}}_f$, the same behavior than in the first test case can be observed, with also a slight decrease of the accuracy in the resulting field $\vec{E}_o$.

Observing Figs. 3c, 3e, 5c and 5e, even if the target field $\vec{E}_o$ is reached in the controlled region Ω_o, it is important to note that the electric field outside this region is totally uncontrolled, meaning that potentially high field levels are produced in the global domain Ω. It is nevertheless possible to add some constraints in (2) to limit the field values. However, by doing so, the accuracy of the generated target field $\vec{E}_o$ could also decrease.

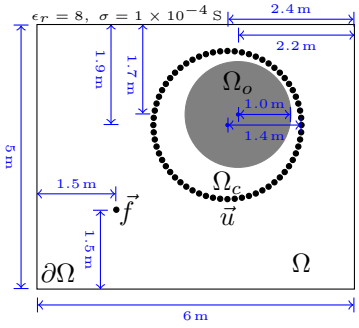

Fig. 4. Configuration of test case 2.

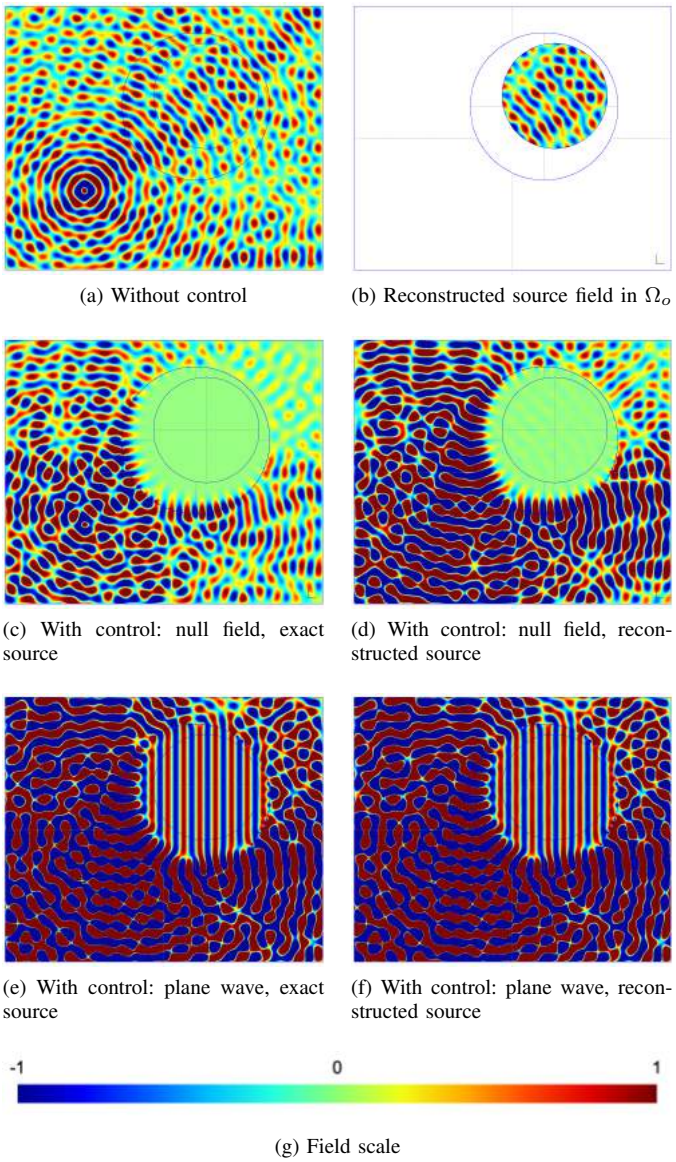

(a) Without control

(b) Reconstructed source field in Ω_o

(c) With control: null field, exact source

(d) With control: null field, reconstructed source

(e) With control: plane wave, exact source

(f) With control: plane wave, reconstructed source

(g) Field scale

Fig. 5. Test case 2: 2D control in a room of the electric field in a target zone using either the exact source field $\vec{E}_f$ ((c),(e)) or the reconstructed field $\tilde{\vec{E}}_f$ ((d),(f)) using 64 sample points.

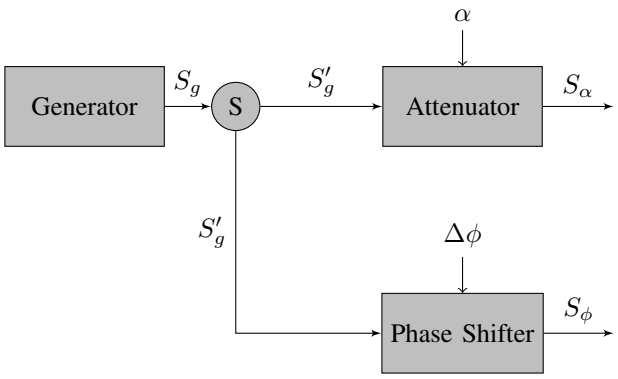

Fig. 6. Block diagram of the source/control generator: S_α is applied to the source while S_ϕ is applied to the control.

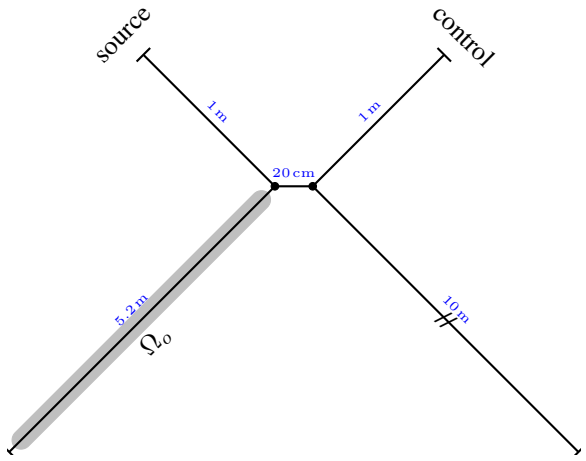

Fig. 7. Configuration of the test case 3.

IV. Experimental Wave Control

For complex environments, many control elements (antennas) are needed to reach the target field $\vec{E}_o$ with a sufficient accuracy, merely because of the sampling criterion to reconstruct the field map $\tilde{\vec{E}}_f$ with the discretized Stratton-Chu formula. Therefore, a practical implementation of the control method in a reverberating room is rather difficult to consider experimentally due to the very high number of needed control elements to be used synchronously (at least in our laboratory, for the time being). On the contrary, we have seen that 1D problems could be controlled by only one or two control elements, depending if the controlled region Ω_o is connected to a boundary or not. As a result, we have focused the experimental applications to 1D cases needing only a single control element. In this case and in the following, the reconstructed field $\tilde{\vec{E}}_f$ using (7) has not been considered since the field can trivially be retrieved using an analytical formula and fitted by a single measurement in Ω_o.

To achieve this, we need phase coherent sources to generate the harmonic signal for both the source and the control element. We have used a single generator Rohde & Schwarz SMF-100A to generate the 1 GHz sinusoidal signal. We have used a 8-bit digital phase shifter (Peregrine Semiconductor DPO PE44820) to produce a phase shifted signal on one channel, and a 6-bit digital step attenuator (Peregrine Semiconductor DSA PE4312) to get an attenuated signal, as shown in Fig. 6. Consequently, both channel signal amplitudes are determined by the output amplitude of the generator, with an extra programmable attenuation α (0.5 dB to 31.5 dB with 0.5 dB step) for the attenuation channel. The phase shifted channel has a phase shift $\Delta\phi$ adjustable from 0° to 360° with 1.4° step.

In the following, experimental and numerical controls are compared through two different one dimensional test cases. The aim of the two test cases is to compare the control values given by numerical method for the corresponding numerical configuration to the values obtained experimentally with a manual search of the minimum field in the controlled region Ω_o (by modifying α and $\Delta\phi$).

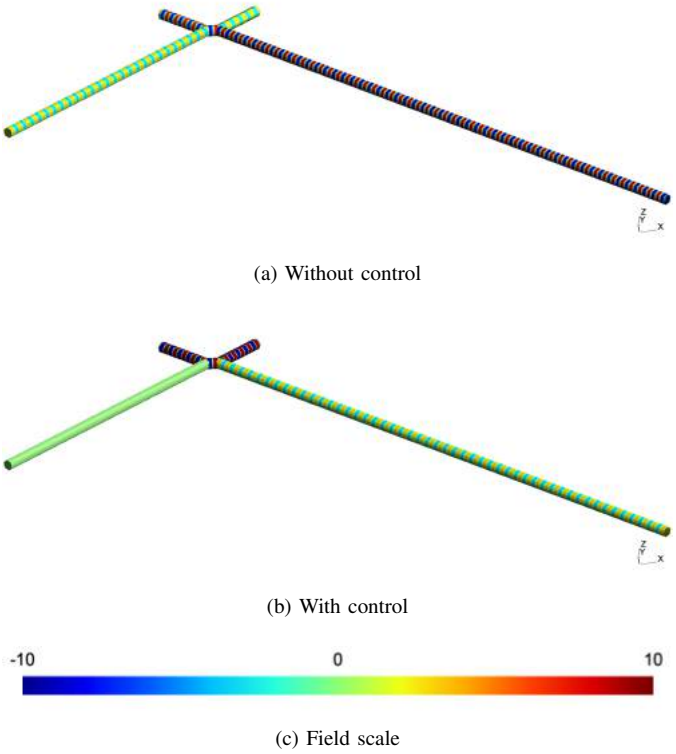

(a) Without control

(b) With control

(c) Field scale

Fig. 8. Test case 3: 1D control in a transmission line of the electric field.

A. Voltage control within a transmission line

Test case 3 consists in a lossy transmission line network, as illustrated in Fig. 7. This "H" shaped transmission line network is traversed by a voltage generated by the harmonic source located at the tip of the upper left leg of the network. The working frequency has been fixed at 1 GHz. The control voltage is applied through the tip of the upper right leg of the network while the controlled region Ω_o has been chosen in the lower left leg.

In Fig. 8, we see that the optimization method is able to find the appropriate control value to reach a zero field state in the controlled region Ω_o located in the lower right leg of the network.

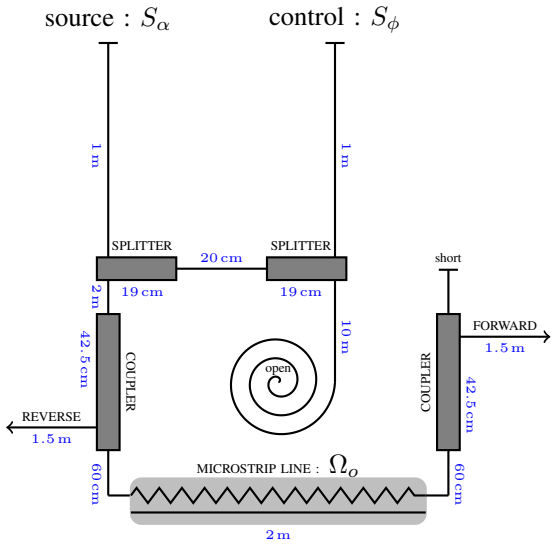

Fig. 9. Configuration of the experimental test case 3.

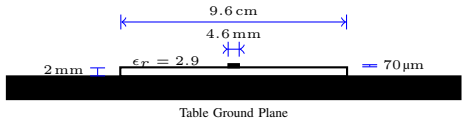

Fig. 10. Crosscut of the microstrip line.

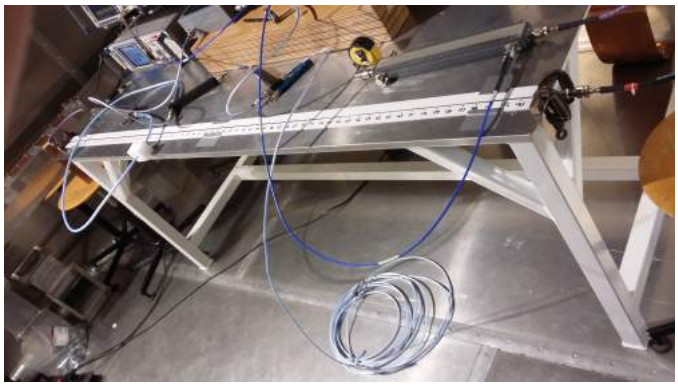

Fig. 11. Experimental setup of the test case 3.

The experimental configuration of test case 3 (Fig. 7) has been slightly modified to cope with some experimental considerations. Indeed, the first problem is that using coaxial cables, measuring the voltage along a portion of a cable is not possible due to its inherent efficient shielding properties. We have thus used a microstrip line to replace the coaxial cable in the controlled region Ω_o, as described in Fig. 9. This has allowed to measure the collected power by a sliding near-field probe standing just on top of the copper track. Although it is certainly not an absolute measurement of the voltage profile in the controlled region, it is definitely the more straightforward image of the voltage along the track since the target voltage is chosen to be zero in the region Ω_o. A crosscut of the used microstrip line is illustrated in Fig. 10. Its parameters were chosen to match at best the characteristic impedance of the used coaxial cables, i.e. $50\,\Omega$, with a total length of $2.0\,\mathrm{m}$. A photograph of the full experimental setup is shown in Fig. 11.

To achieve the control along the microstrip line, we have manually searched the best set of parameters α and $\Delta\phi$ to apply to reach the lowest measured voltage collected at each coupler, positioned at the beginning and at the end of the microstrip line. The best control couple values was $4.0\,\mathrm{dB}$ for α and $234°$ for $\Delta\phi$. The voltage along the microstrip line before and after applying the control is displayed in Fig. 12. By applying the control voltage, the measured voltage along the microstrip using a near-field probe is globally $30\,\mathrm{dB}$ in average lower than without applying the control. We also see that we have not reached the noise level measured while the source and the control are turned off. It means that the value of the control could certainly be refined but here, we are probably limited by the digital accuracy of our equipment ($0.5\,\mathrm{dB}$ for α and $1.4°$ for $\Delta\phi$).

In comparison, numerically, the couple of values of the control to apply was found to $4.5\,\mathrm{dB}$ for α and $232°$ for $\Delta\phi$ which is rather near the best experimental control pair.

B. *Electric field control within a waveguide*

Test case 4 aims to control the electric field within a waveguide network. Although a waveguide has a 3D geometry, we have made sure to obtain a one dimensional transmission line behavior by using the appropriate geometrical parameters. Test case 4 employs a waveguide section of $18\,\mathrm{cm} \times 15\,\mathrm{cm}$ for a frequency of $1\,\mathrm{GHz}$, allowing to propagate the TE_{01} mode having a single vertical electric field component. Using the frequency of $1\,\mathrm{GHz}$ also allows the TE_{11} to propagate, but due to technical considerations, lower frequencies could not be used. The rather large dimensional values of the waveguide network, summarized in Fig. 14 may look a bit odd, but the explanation is strictly experimental: we wanted to compare the numerical results with a true experimental version of the same test case, and to be able to perform the measurements inside the waveguide, we have thus chosen large sections and lengths.

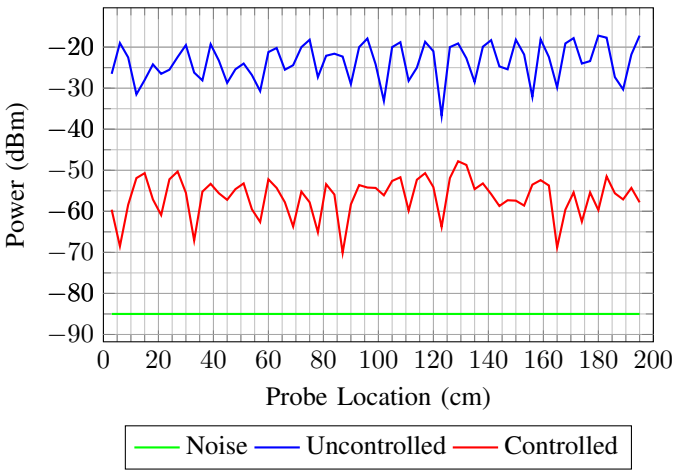

Fig. 12. Experimental results of the voltage control within the microstrip line.

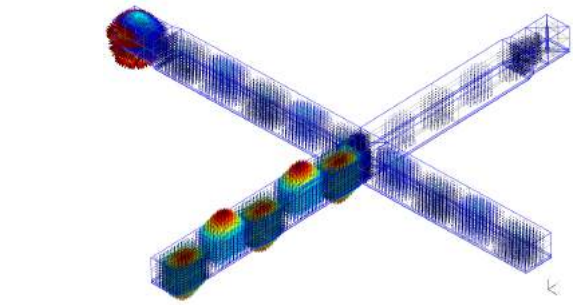

(a) Without control

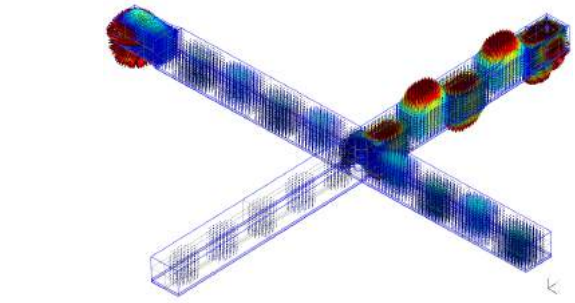

(b) With control

(c) Field scale

Fig. 13. Test case 4: 3D control in a waveguide of the electric field.

The waveguide is fed by two monopoles ($\lambda/4$) to impose the source and the control fields. A metallic cylinder has been placed in the center of the network, to complexify power distribution in each leg of the network.

The results from test case 4, displayed in Fig. 13, show that the applied control reduces significantly the resulting field in the region Ω_o, when a null target electric field $\vec{E}_o$ is chosen.

The corresponding experimental test case is a direct implementation of the numerical test case 4, presented above. As in the previous experimental test case, we had to proceed to some small modifications to be able to measure the field inside the controlled region of the waveguide Ω_o. The waveguide network is composed of different aluminium stretches mechanically fastened together with several clamps. A slit has been cut in the middle of Ω_o to insert a moving antenna probe to measure the received power along the controlled part of the waveguide. A soft lip electromagnetic seal covers the slit to maintain shielding while allowing the probe displacement. The probe sensor is a monopole antenna of the same type as the source and the control feed elements. The working frequency was fixed at $1.0\,\mathrm{GHz}$. The resulting configuration is summarized in Fig. 14 and in Fig. 15 for the practical setup.

The best control pair has been manually identified to find the

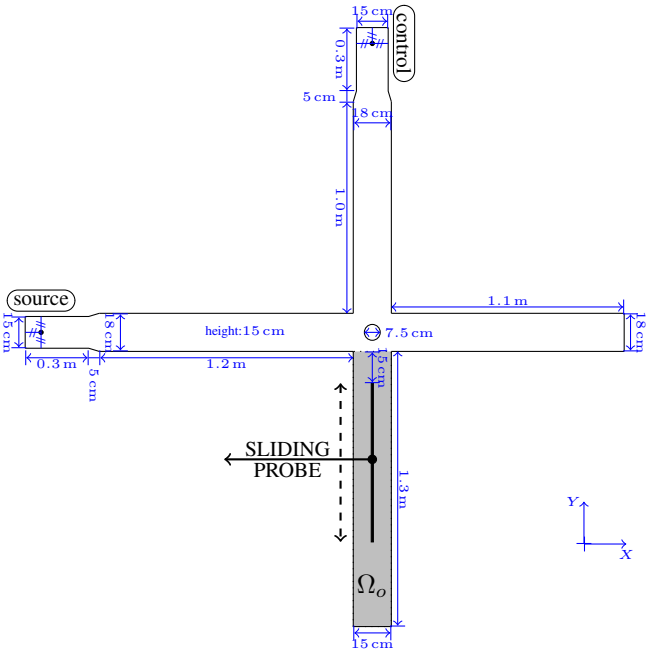

Fig. 14. Configuration of the test case 4.

minimum field values along the measurement slit in the waveguide. The values $\alpha = 17.5\,\mathrm{dB}$ and $\Delta\phi = 188°$ were found, and the corresponding measured power inside Ω_o is plotted in Fig. 16, as well as the power before applying any control value and the noise without any source feeding the waveguide. The result is globally interesting since the measured power is reduced by about $25\,\mathrm{dB}$ in average in the controlled region. It is not as good as the previous experimental result concerning the microstrip line. This is mainly probably due to the non vertical TE_{10} mode component that the system is unable to compensate. In our opinion, another possible reason could be induced by the low field strength caused by the control field in the controlled leg of the waveguide compared to the field strength of the source. With an attenuation of $\alpha = 17.5\,\mathrm{dB}$, it means that the level of the generated field (source and control) was already low to have the best sensitivity of the spectrum when varying the control value.

Finally, comparing the experimental control pair with the numerical one ($17.1\,\mathrm{dB}$ for α and $195°$ for $\Delta\phi$), it appears that the matching is quite close.

These two test cases 3 and 4 have shown that the numerical method could accurately find the optimal control values to apply. Based on these promising results for single control element environments, we are confident in applying the same method for multiple control elements, for which adjusting the control values manually become too cumbersome but nevertheless covers a wider range of applications. Using 32 control elements, it could be possible to sample and control experimentally a spherical region of about $80\,\mathrm{cm}$ of diameter in free-space or in a reverberating environment. With an accurate numerical model, the need of sampling $\vec{E}_f$ in Ω_c could become useless, which would also simplify the experimental control procedure.

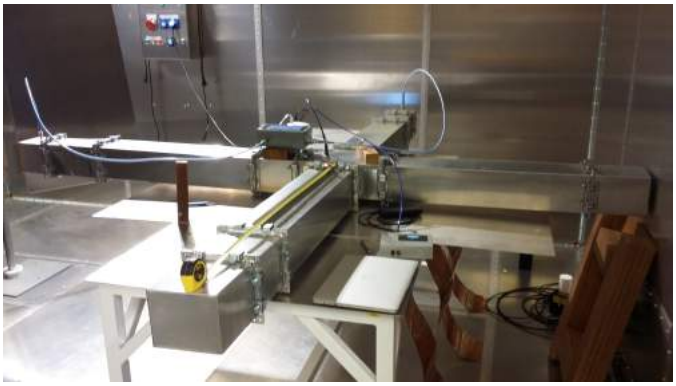

Fig. 15. Experimental setup of the test case 4.

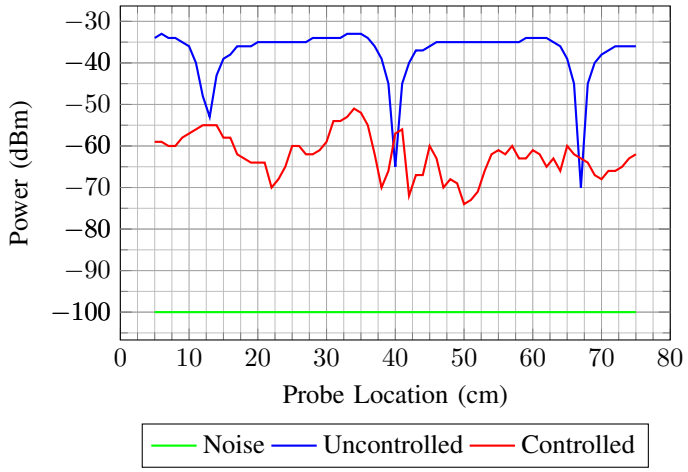

Fig. 16. Experimental results of the field control within the waveguide.

V. Conclusions

We have proposed a method to impose an arbitrary field in a part of an environment subject to the field generated by one or more noise sources, by acting on control values located at determined source locations. This method relies on a well-known constrained optimization method for the electromagnetic wave equation. An integral formula has also been used to be able to reconstruct the field map to cancel on a region from its boundary. The proposed numerical test cases have shown accurate reconstruction of the target field map in the controlled region, with a slight decrease of accuracy when considering reconstructed noise field maps. However, this formula requires to sample the electric and magnetic fields to be compensated on the boundary of the targeted controlled zone, which is a limitation and remains an open topic. More interestingly, the experimental test cases directly transposed from the numerical test cases have shown very close results compared to the computed single source control by the numerical models which is very promising to extend the method to more complex test cases with multiple control elements to drive.

References

[1] J. Lions, "Exact controllability, stabilization and perturbations for distributed systems," *SIAM Review*, vol. 30, no. 1, pp. 1–68, 1988. [Online]. Available: http://dx.doi.org/10.1137/1030001

[2] R. Glowinski, C.-H. Li, and J.-L. Lions, "A numerical approach to the exact boundary controllability of the wave equation (i) Dirichlet controls: Description of the numerical methods," *Japan Journal of Applied Mathematics*, vol. 7, no. 1, pp. 1–76, 1990. [Online]. Available: http://dx.doi.org/10.1007/BF03167891

[3] J. E. Lagnese, "Exact boundary controllability of Maxwell's equations in a general region," *SIAM Journal on Control and Optimization*, vol. 27, no. 2, pp. 374–15, 03 1989. [Online]. Available: https://search.proquest.com/docview/925975700?accountid=14630

[4] M. Darbas, O. Goubet, and S. Lohrengel, "Exact boundary controllability of the second-order maxwell system: Theory and numerical simulation," *Computers & Mathematics with Applications*, vol. 63, no. 7, pp. 1212 – 1237, 2012. [Online]. Available: http://www.sciencedirect.com/science/article/pii/S0898122111011023

[5] A. Cozza, "Emulating an anechoic environment in a wave-diffusive medium through an extended time-reversal approach," *Antennas and Propagation, IEEE Transactions on*, vol. 60, no. 8, pp. 3838–3852, 2012.

[6] J. Benoit, C. Chauvière, and P. Bonnet, "Source identification in time domain electromagnetics," *Journal of Computational Physics*, vol. 231, no. 8, pp. 3446 – 3456, 2012. [Online]. Available: http://www.sciencedirect.com/science/article/pii/S0021999112000411

[7] M. Spirlet, "Correction of electromagnetic measurements and active shaping of electromagnetic fields in complex and reverberating environments," Ph.D. dissertation, 2018. [Online]. Available: http://hdl.handle.net/2268/221244

[8] P. Courilleau, T. H. Molinaro, and I. G. Stratis, "On the controllability of time-harmonic electromagnetic fields in chiral media," *Advances in Mathematical Sciences and Applications*, vol. 16, no. 2, p. 491, 2006.

[9] K. Ito and K. Kunisch, *Lagrange Multiplier Approach to Variational Problems and Applications*. Society for Industrial and Applied Mathematics, 2008. [Online]. Available: http://epubs.siam.org/doi/abs/10.1137/1.9780898718614

[10] Leugering, *Constrained optimization and optimal control for partial differential equations.*, G. Leugering, S. Engell, A. Griewank, M. Hinze, R. Rannacher, V. Schulz, M. Ulbrich, and S. Ulbrich, Eds. Basel: Birkhäuser, 2012.

[11] H. Maurer and H. D. Mittelmann, "Optimization techniques for solving elliptic control problems with control and state constraints: Part 1. boundary control," *Computational Optimization and Applications*, vol. 16, no. 1, pp. 29–55, 2000. [Online]. Available: http://dx.doi.org/10.1023/A:1008725519350

[12] ——, "Optimization techniques for solving elliptic control problems with control and state constraints. part 2: Distributed control," *Computational Optimization and Applications*, vol. 18, no. 2, pp. 141–160, 2001. [Online]. Available: http://dx.doi.org/10.1023/A:1008774521095

[13] C. Bardos, G. Lebeau, and J. Rauch, "Sharp sufficient conditions for the observation, control, and stabilization of waves from the boundary," *SIAM Journal on Control and Optimization*, vol. 30, no. 5, pp. 1024–42, 09 1992. [Online]. Available: https://search.proquest.com/docview/925912210?accountid=14630

[14] M. Selvanayagam and G. V. Eleftheriades, "An active electromagnetic cloak using the equivalence principle," *IEEE Antennas and Wireless Propagation Letters*, vol. 11, pp. 1226–1229, 2012.

[15] F. G. Vasquez, G. W. Milton, and D. Onofrei, "Active exterior cloaking for the 2d laplace and helmholtz equations," *Phys. Rev. Lett.*, vol. 103, p. 073901, 8 2009. [Online]. Available: https://link.aps.org/doi/10.1103/PhysRevLett.103.073901

[16] M. Selvanayagam and G. V. Eleftheriades, "Experimental demonstration of active electromagnetic cloaking," *Phys. Rev. X*, vol. 3, p. 041011, 2013. [Online]. Available: https://link.aps.org/doi/10.1103/PhysRevX.3.041011

[17] D. Schurig, J. J. Mock, B. J. Justice, S. A. Cummer, J. B. Pendry, A. F. Starr, and D. R. Smith, "Metamaterial electromagnetic cloak at microwave frequencies," *Science*, vol. 314, no. 5801, pp. 977–980, 2006. [Online]. Available: http://science.sciencemag.org/content/314/5801/977

[18] E. Casas, "Second order analysis for bang-bang control problems of PDEs," *SIAM Journal on Control and Optimization*, vol. 50, no. 4, pp. 2355–2372, 2012. [Online]. Available: https://search.proquest.com/docview/1034868642?accountid=14630

[19] M. Bergounioux, K. Ito, and K. Kunisch, "Primal-dual strategy for constrained optimal control problems," *SIAM Journal on Control and Optimization*, vol. 37, no. 4, pp. 1176–19, 1999. [Online]. Available: https://search.proquest.com/docview/925817182?accountid=14630

[20] E. Casas, "Control of an elliptic problem with pointwise state constraints," *SIAM Journal on Control and Optimization*,

vol. 24, no. 6, pp. 1309–10, 11 1986. [Online]. Available: https://search.proquest.com/docview/926026152?accountid=14630

[21] ——, "Boundary control of semilinear elliptic equations with pointwise state constraints," *SIAM Journal on Control and Optimization*, vol. 31, no. 4, pp. 993–14, 07 1993. [Online]. Available: https://search.proquest.com/docview/925868452?accountid=14630

[22] E. Casas, F. Troltzsch, and A. Unger, "Second order sufficient optimality conditions for some state-constrained control problems of semilinear elliptic equations," *SIAM Journal on Control and Optimization*, vol. 38, no. 5, pp. 1369–23, 2000. [Online]. Available: https://search.proquest.com/docview/925816040?accountid=14630

[23] P. Monk, *Finite Element Methods for Maxwell's Equations*, ser. Numerical mathematics and scientific computation. Clarendon Press, 2003.

[24] J. A. Stratton and L. J. Chu, "Diffraction theory of electromagnetic waves," *Phys. Rev.*, vol. 56, pp. 99–107, 7 1939. [Online]. Available: http://link.aps.org/doi/10.1103/PhysRev.56.99

[25] P. Dular, C. Geuzaine, F. Henrotte, and W. Legros, "A general environment for the treatment of discrete problems and its application to the finite element method," *IEEE Transactions on Magnetics*, vol. 34, no. 5, pp. 3395–3398, 9 1998.

[26] C. Geuzaine and J.-F. Remacle, "Gmsh: A 3-d finite element mesh generator with built-in pre- and post-processing facilities," *International Journal for Numerical Methods in Engineering*, vol. 79, no. 11, pp. 1309–1331, 2009. [Online]. Available: http://dx.doi.org/10.1002/nme.2579

[27] E. Joy and D. Paris, "Spatial sampling and filtering in near-field measurements," *Antennas and Propagation, IEEE Transactions on*, vol. 20, no. 3, pp. 253 – 261, 05 1972.